Control of a gripper finger actuated by a pneumatic muscle: new schemes based on a model-free approach

Pol Hamon, Loïc Michel, Franck Plestan, Damien Chablat

Control of a gripper finger actuated by a pneumatic muscle: new schemes based on a model-free approach

Pol Hamon [*,**] **Loïc Michel** [**] **Franck Plestan** [**]
Damien Chablat [**]

[*] *Armor Meca Developpement, 22490 Pleslin-Triavou, France, (Pol.hamon@armor-meca.com)*
[**] *Nantes Université, Ecole Centrale Nantes, CNRS, LS2N, UMR CNRS 6004, F-44000 Nantes (Loic.Michel@ec-nantes.fr, Franck.Plestan@ec-nantes.fr, Damien.Chablat@cnrs.fr)*

Abstract: In this paper, model-free based control strategies are applied to a finger of a gripper activated by Mckibben pneumatic muscles. In order to emulate the grasping phase of an object using a simple finger, a "hybrid" type model-free based control strategy is proposed to manage the effort control phase, and the object release phase. The strategy is divided into a phase of approach to the object with a speed control, then a phase of contact with the object for which a control of the effort is applied to maintain a controlled pressure on the object, and finally, a release phase for which the withdrawal of the object is controlled in position. An experimental setup is introduced to experiment with the control strategies on a single phalanx finger.

Keywords: Robotic gripping system, pneumatic muscle, model-free control.

1. INTRODUCTION

One of the great challenges of industrial robotics is to manipulate a large number of objects with varied and complex shapes and different masses reword safety. For this reason, a new under-actuated hand with more degrees of freedom has been developed [Hamon et al. (2021)]. To operate this new gripper, pneumatic muscles have been chosen: indeed, the coupling between pressure, contraction, and effort can be advantageous to achieve under-actuated gripping [Birglen et al. (2010)]. Furthermore, the high effort-mass ratio of pneumatic muscles is an interesting feature when an object is grabbed.

The transition from free finger movement to holding the object is intuitive. However, there are two very different situations, which use two kinds of feedback: proprioception and touch. In the human case, the vision allows anticipating the transition between these two situations. If there is no visual information, it is necessary to recreate an intuitive blind grasp. Solutions have been proposed in [Sgarbi and Detriche (1989)] and [Xu (2013)] with an alternation between motion phase and grabbing phase. Notice that similar solutions can be found for walking robots [Yeh et al. (2010)]. However, it introduces the problem of reliable and responsive contact detection; as an example, in [Birglen and Gosselin (2004)], fuzzy logic is used for a smooth transition between the two sensors.

In the current paper, a solution for a gripper with velocity and force control without force detection is proposed; the gripper being actuated by a Mckibben pneumatic muscle.

Few contributions have been made concerning the control of pneumatic artificial muscles (PAM) used as actuators [Takosoglu et al. (2016); Tondu (2012)] for a finger. Standard Ziegler-Nichols method has been proposed in [Takosoglu (2020)] to tune a PID controller for the position control purpose. Similarly, a PID controller tuned by Simulated Annealing method has been considered in [Scaff et al. (2018)] regarding a positioning system. In [Godage et al. (2018)], an experimental PID control based on a specific hysteresis model has been proposed. Such strategies require the identification of a model: thus, self-identification-based control using neural networks has been proposed in [Thanh and Ahn (2006); Pham Huy Anh (2010); Zhao et al. (2015); Zhong et al. (2018)]. A recent contribution to illustrate the feasibility of a positionning system using a grey-box-based identification modeling using neural networks and sliding mode control in real-time applications has been proposed in [Ba et al. (2016)].

To overcome the difficulty of modeling, in the current paper, a strategy based on the model-free control approach [Fliess and Join (2013)] is proposed to solve the problem of controlling the movement of a gripper finger actuated by pneumatic muscles, for gripping a wide variety of different objects, while limiting the identification process. The model-free control approach [Fliess and Join (2021)] can be considered as an alternative to the standard PI and PID controls, that does not require any prior knowledge of the plant, and it is straightforward to tune. Its usefulness in many situations, including severe non-linearities and

[⋆] The work has been supported by the French National Association for Research in Technology (ANRT) through the CIFRE 2019/27 and Armor Meca Developpement.

time-varying properties, has been demonstrated through successful applications: see, e.g., [Bara et al. (2018); Fliess and Join (2013); Hamiche et al. (2019)]. In particular, some applications have been dedicated to the control of quadrator position [Bekcheva et al. (2018); Younes et al. (2014)] or machine tool positioning systems [Villagra et al. (2020)]. This kind of approach is computationally efficient, easily deployable even on small embedded devices, and can be implemented in real-time since it requires very light computations.

This paper is structured as follows. Section 2 states the control problem. Section 3 presents the control strategies and Section 4 describes the experimental setup used for the experiment. In Section 5, principles of model-free control are presented. In Section 6, experimental results illustrate the control strategy. Section 7 gives some concluding remarks.

2. PROBLEM STATEMENT

The description of the different phases of operation is made in this section and in Figure 1. These phases allow to define the control strategies.

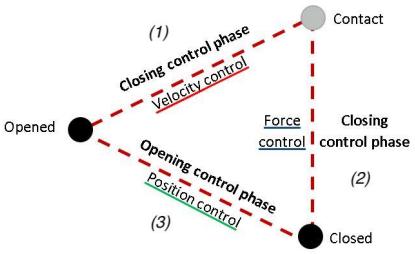

Fig. 1. Control phases between the open and closed positions.

Closing control step. In this step, the objective is to grab the part. This step is divided into two distinct phases:

- *Phase 1* hangs over the finger toward the object by controlling the speed to reach the object;
- *Phase 2* makes the contact with the object maintained under a constant controlled effort.

In Phase 1, the motion is as fast as possible whereas, in Phase 2, the objective is to achieve a target in force without overshoot, especially during the contact phase. This fact limits the speed of Phase 1 according to the expected effort reference. In our case, this relationship between speed and force reference is constant and is fixed, so that there is no overshoot on the force target.

Opening control step. The opening of the gripper must be controlled in position because one of the objectives of the gripper will be to place the objects correctly, close to each other, without impacting the objects around. This leads to Phase 3.

- *Phase 3* opens the finger, breaks the contact, and stabilizes the position to a controlled value.

3. CONTROL STRATEGIES FOR CLOSING AND OPENING PHASES

Closing with switching control. The first solution consists in using an existing scheme [Sgarbi and Detriche (1989); Xu (2013)] including a contact detection that gives a hybrid control structure (Figure 2): the control is switching between a speed one (Phase 1) to a force one (Phase 2), the switching being made when the contact is trully detected. Afterwards, the loss of contact must be detected if the part moves due to an effort before being immobilized in the clamp. G_1 and G_2 gains (Figure 2) normalize the signal and allow the scaling gain between speed and force. To adjust the gain G_1, a maximum approach speed without exceeding the effort during contact is considered. Notice that the use of a hybrid control approach makes the stability proof more complex.

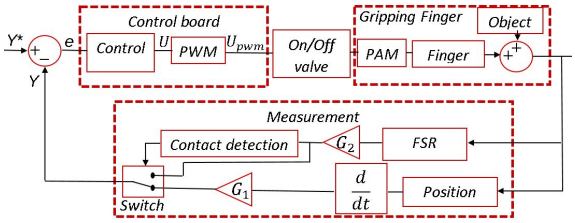

Fig. 2. Hybrid closed-loop scheme for Phases 1 and 2.

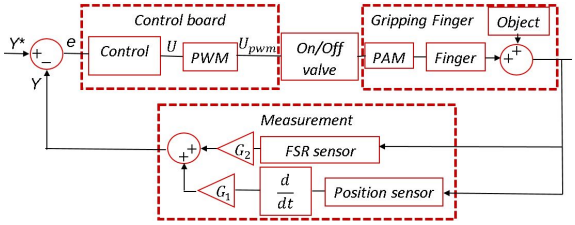

Fig. 3. Closed-loop scheme with a single reference for Phases 1 and 2.

Closing with a speed+effort control. Another alternative is the use of a single reference, defined as a combination of speed and force signals in order to avoid contact detection (see Figure 3). In Phase 1, the force is close to zero, whereas in Phase 2 the velocity is close to zero; the transition between the two phases is determined by the stiffness of the system. Figure 3 presents the corresponding closed-loop scheme.

Opening by tracking of the angular position: Phase 3 consists of opening the finger in order to cancel the effort on the object while stabilizing the position of the finger. Phase 3 switches the reference to a position reference when the contact with the object is lost and thus the finger tracks a position reference. Figure 4 presents the corresponding closed-loop scheme.

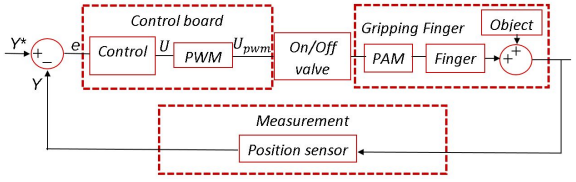

Fig. 4. Closed-loop scheme for Phase 3.

4. EXPERIMENTAL SETUP

In this section, the experimental setup used to evaluate the performances of the proposed control scheme is presented.

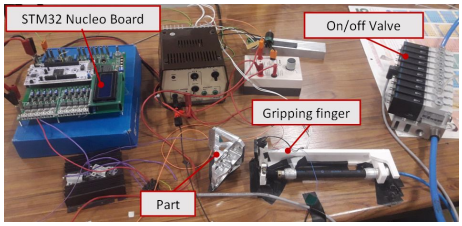

Fig. 5. Test bench.

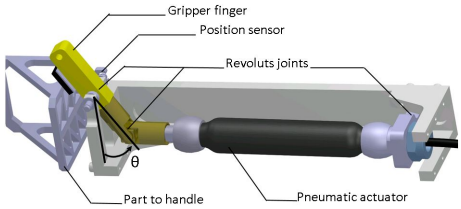

Fig. 6. CAD of a finger with a pneumatic muscle.

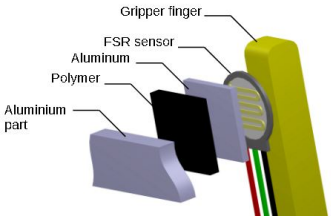

Fig. 7. CAD of the contact surface.

Notice that this setup has been designed as a preliminary step, the future goal being to propose a control scheme for a multi-finger gripper [Hamon et al. (2021)] that is currently under design. This future system will equip an industrial robot: that is why only tools (basic sensors, ...) that are easy to find and available on the market have been used for the set-up.

4.1 Test bench

The test bench (Figure 5) has been built to develop the control solution with a single gripping finger in order to neglect the interactions between the fingers during a grip. Moreover, all the elements are fixed to the round.

The test bench (Figure 6) consists of a Mckibben pneumatic muscle (Festo DMSP-10-130N-AM-CM) which activates a gripping finger referenced with a θ angle. The return of the finger to its initial position is ensured by the stiffness of the pneumatic muscle. The parts of the finger are made from machined aluminum whereas the gripping surface is made from polymer (Figure 7) that makes the contact softer and increases the sliding coefficient.

4.2 On-off valve

The control drives the signal sent to the ON/OFF 5/2 solenoid valve that drives the pneumatic pressure to the Mckibben muscle. The valve is driven using a variable duty-cycle (conversion of the output of the control as a duty-cycle), the duty-cycle being controlled between 0.5 and 1, since, below 0.5, the pressure is not maintained in the PAM. Due to the dynamics of the PAM with a cut-off frequency of 150 Hz, the valves are driven at a constant frequency of 200 Hz.

4.3 Measurement

The measurement is provided by two sensors: an angle sensor (Magnetic Encoder RLS RM08) integrated in the rotation axis of the finger and a force sensor FSR (IE FSR X 402) between the polymer/aluminum contact surface and the finger (Fig. 7). These two sensors provide analog 0-5V signals. These latter are filtered thanks to a standard 20 Hz-fourth-order Butterworth filter [1]. The velocity is obtained by the differentiation of the position signal.

4.4 Control hardware

The control is managed owing to an STM32 Nucleo board H743ZI2 allowing a 16-bit ADC acquisition as well as the possibility to monitor the signals in real-time on the computer. The valve is updated at 200 Hz through a PWM modulation and the control is updated at 20 kHz ; the lift signal is acquired in the Nucleo board to be used as the control input sampled at 20 kHz.

5. RECALLS ON MODEL-FREE CONTROL

As previously introduced, the objective here is to propose a new control scheme that requires a very reduced effort for the identification/modeling while keeping high performances in terms of accuracy and robustness. A solution is the so-called "model-free control" approach that is detailed in [Fliess and Join (2013)]. Its usefulness in many situations, including compensating severe non-linearities and time-varying reference signals, has been demonstrated. The corresponding intelligent controllers are much easier to implement and to tune than PID controllers which are today the main tool in industrial control engineering (see, e.g., [Åström and Murray (2008)]).

5.1 The ultra-local model

The main ideas of model-free control are explained in the sequel. This approach is based on an ultra-local model in the sense that it is well-adapted during a very short time. From this ultra-model, a linear controller can be designed. A key point is the capability of the controller to be adapted to the evolution of the ultra-local model given that very reduced information is available.
The dynamic description of the plant [2] is made by the following *ultra-local model* of order 1, denoted F such as

$$\boxed{\dot{y} = F + \alpha u} \tag{1}$$

where

- y and u are respectively the control and output of the system,
- $\dot{y}$ designates the time-derivative of y,
- the constant $\alpha \in \mathbb{R}$ is chosen by the practitioner such that $\dot{y}$ and αu are of the same magnitude. Therefore, α does not need to be precisely estimated.

As previously mentioned, equation (1) is only valid during a short time-lapse, hence the *ultra-local* term. It must be continuously updated.

[1] The *butter* function of Matlab ® is used to perform a discrete fourth order low pass filtering.
[2] For sake of simplicity and clarity, the system is supposed to be a SISO (single-input single-output) one.

5.2 Control design

As a trivial introduction, supposing that F is perfectly known, considering the following controller

$$\boxed{u = -\frac{F - \dot{y}^* + K_P e}{\alpha}} \tag{2}$$

where

- y^* is the output reference trajectory;
- $e = y - y^*$ is the tracking error;
- K_P is a tuning gain [3];

then the closed-loop system behavior is governed by the following equation

$$\dot{y} = \dot{y}^* - K_P e \tag{3}$$

that gives $\dot{e} = -K_P e$. However, F is not available and forces to consider another control strategy. To make an accurate analysis, and given that the control law will be implemented in discrete time, consider now the following *ultra-local* discrete model at the k-th time

$$\left.\frac{\mathrm{d}y}{\mathrm{d}t}\right|_k = F_k + \alpha u_k \tag{4}$$

for which the control u_k has to be determined. A solution called "intelligent" digital P-controller [Michel et al. (2010)] reads as (one supposes that the reference trajectory y^* is well-known)

$$\boxed{u_k = u_{k-1} - \frac{1}{\alpha}\left(\left.\frac{\mathrm{d}y}{\mathrm{d}t}\right|_{k-1} - \left.\frac{\mathrm{d}y^*}{\mathrm{d}t}\right|_k\right) - K_p(y|_k - y^*|_k)} \tag{5}$$

Considering the ultra-local model at $k-1$-time

$$\left.\frac{\mathrm{d}y}{\mathrm{d}t}\right|_{k-1} = F_{k-1} + \alpha u_{k-1} \tag{6}$$

one gets

$$u_{k-1} = \frac{1}{\alpha}\left(\left.\frac{\mathrm{d}y}{\mathrm{d}t}\right|_{k-1} - F_{k-1}\right) \tag{7}$$

Replacing (7) in (5), and applying this latter to (4), one gets

$$\left.\frac{\mathrm{d}y}{\mathrm{d}t}\right|_k - \left.\frac{\mathrm{d}y^*}{\mathrm{d}t}\right|_k = -\alpha\, K_p(y|_k - y^*|_k) + F_k - F_{k-1} \tag{8}$$

This last dynamics is stable if the term $F_k - F_{k-1}$ is small enough. The following hypothesis can be made: the ultra-local model is valid only over a very short time during which the perturbation has changed very little. Then, $F_k \approx F_{k-1}$ that makes equation (8) converging towards a vicinity of 0 (this asssumption imposes a high sampling rate of the control).

Remarks.

- The presence of u_{k-1} in the definition of u_k allows, by an indirect way, to take into account the unknown term F_{k-1}.
- The control law (5) requires the time derivative of y. Its estimation is performed by using an Euler-method based differentiator.

[3] Practically, α and K_p can be tuned following e.g. the proposed procedure described in [d'Andréa Novel et al. (2010)].

5.3 Illustrative application: position tracking of the finger

In order to illustrate the model-free control approach, consider here the tracking of the angular position [4] of the finger actuated by the pneumatic muscle: the output y is the angular position of the finger whereas the reference y^* is a sinusoidal one. The control drives the signal sent to the solenoid valves to release or block the pressurized air. The proposed control strategy replaces both the mathematical models of the finger and the PAM [Tondu and Lopez (2000)] by a "phenomenological" and ultra-local model valid only over a short period of time. Remark that the term F includes all the uncertainties, perturbations and modeling errors.

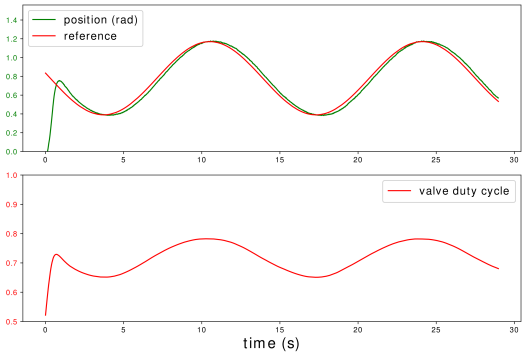

Fig. 8. Tracking of a sine reference.

Figure 8 depicts the controlled position according to the reference where the coefficients of (5) are set to $\alpha = 30$ and $K_p = 8$. The choice of these parameters has been made in order to get a good behavior of the closed-loop system. It is clear that the tracking is satisfactory even if a delay appears probably due to the discretization (some improvements could be obtained by using a more effective differentiator). Finally, the performances are acceptable given that there is no modeling effort.

6. EXPERIMENTAL RESULTS

The technical specifications are defined in Section 2 and Section 3 for the different phases, and the experimental set-up is described in Section 4. It yields that the control strategy is applied for Phases 1, 2 and 3, according to the chosen closed-loop schemes, involving the same model-free control law with different feedback parameters.

- *Hybrid closed-loop scheme-Phases 1 and 2.* (Figure 2). In this case, the system output y is either the finger angular velocity or the force, that gives (with θ the angular position of the finger and f the force detected by the finger)

$$y = \begin{cases} G_1\dot{\theta} & \text{when there is no contact} \\ G_2 f & \text{when there is contact} \end{cases} \tag{9}$$

- *Closed-loop scheme with a single reference-Phases 1 and 2.* (Figure 3). In this case, the system output y is a composition between the angular velocity $\dot{\theta}$ and the force f that is

$$y = G_1\dot{\theta} + G_2 f \tag{10}$$

[4] This case is similar to Phase 3 (see Figure 4).

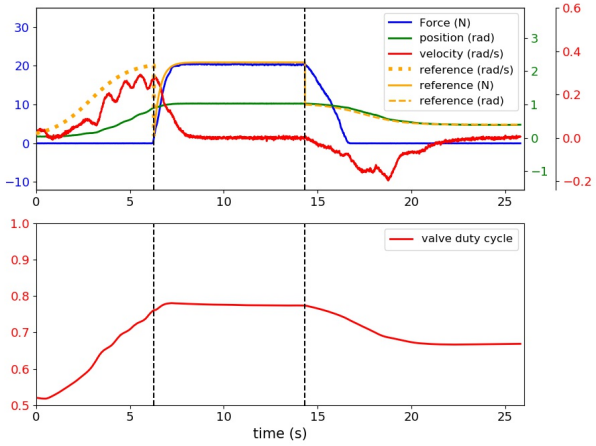

Fig. 9. **Scenario 1.** Experimental results with force reference fixed at 20 N and with contact detection.

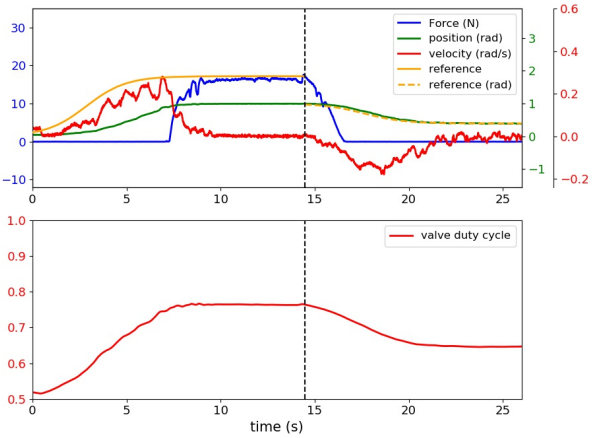

Fig. 10. **Scenario 2.** Experimental results with force reference=15 N without contact detection.

- *Closed-loop scheme for the opening-Phase 3.* (Figure 4). In this case, the system output y is the angular position θ that is

$$y = \theta \tag{11}$$

The goal of the experimentation is to evaluate the performance of the control when the system is tracking the desired trajectory. For this purpose, the reference curve is constructed from sigmoid ones whose starting point is the last state of the system before the activation of the control phase.

Three scenarios have been used to make all the steps displayed by Figure 1:

- **Scenario 1 (Figure 9).** This scenario evaluates the controller by considering the output (9) that gives: tracking of angular velocity $\dot{\theta}$ reference trajectory (dotted yellow line); then after contact detection, force f reference trajectory (solid yellow line); then, for opening phase, angular position θ reference trajectory (dashed yellow line). The force reference is fixed at $20N$.
- **Scenario 2 (Fig. 10).** This scenario evaluates the controller considering the output (10) that gives: tracking of a reference composed by the angular velocity $\dot{\theta}$ and the force f (solid yellow line); then, for opening phase, angular position θ reference trajectory (dashed yellow line). The force reference is fixed at $15N$.
- **Scenario 3 (Fig. 11).** This scenario is similar to Scenario 2, with a force reference fixed at $25N$.

In the three scenarios, the opening phase starts at $t = 14.5$ sec [5], the position reference being defined to reach $\theta = 0.4$ rad. The control parameters have been tuned in order to achieve good performances (a compromise between robustness, accuracy, transient behaviour): $\alpha = 0.1$, $K_p = 1.2$. The scale gains $G_1 = 58.3$ s.rad^{-1} and $G_2 = 1$ N^{-1} are used for Phases 1 and 2. For the opening control phase, the parameters are fixed at $\alpha = 1$ and $K_p = 4.8$.

In each scenario, the control starts to grasp the object, the first (part of) reference consisting to drive the velocity

[5] In Figures 9-10-11, the detection time is denoted by a vertical dashed black line.

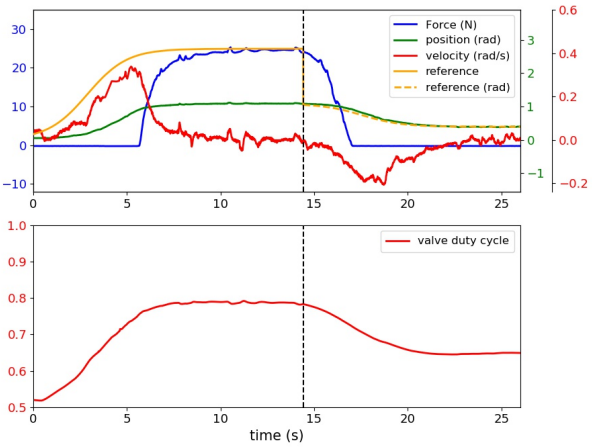

Fig. 11. **Scenario 3.** Experimental results with force reference=25 N without contact detection.

while there is no effort. It appears that, in both cases, the target is not exactly reached and the signal is oscillating (solid red lines). Notice that it is not critical in the current applications because the objective is not to track precisely a velocity reference trajectory, but to get the contact with the object at a low velocity to avoid overshoot; more reliable speed tracking would allow a faster speed.
Once the contact with the object is made, the effort reaches the reference in all three scenarios (solid blue lines); however, in Scenarios 2 and 3, it appears that the force has higher variations than in Scenario 1. This is because the reference for Scenarios 2 and 3 is also depending on the velocity signal that is derived from the position measurement. This fact, coupling with a low-cost position sensor, introduces noise in the reference and then oscillations of the output. However, recall that the hybrid approach of Scenario 1 requires an accurate proof of stability that is more complex.
The coupling between velocity and force has other effects such as the response time to the force reference: in Scenarios 2 and 3, it is greater than the scenario with contact detection. However, the design of a more stiff test bench could reduce this response time but would impose a lower speed of displacement so as not to overshoot in effort on contact.

Finally, concerning the opening, the control allows an efficient tracking (solid green lines after the detection), that remains close to the object to be safe and ready to remove the gripper.

7. CONCLUDING REMARKS

In this work, a model-free control has been applied to a control scheme allowing velocity, force, and position control of one finger of a gripper activated by a pneumatic muscle. Different scenarios have been presented with different force targets to illustrate the feasibility and the performances of the control solution. The analysis shows that a control scheme without contact sensors can be used. This property is very interesting for industrial use. Future work will extend the control strategy for grasping real objects with an under-actuated three-finger gripper.

REFERENCES

Ba, D.X., Dinh, T.Q., and Ahn, K.K. (2016). An integrated intelligent nonlinear control method for a pneumatic artificial muscle. *IEEE/ASME Transactions on Mechatronics*, 21(4), 1835–1845.

Bara, O., Fliess, M., Join, C., Day, J., and Djouadi, S.M. (2018). Toward a model-free feedback control synthesis for treating acute inflammation. *Journal of Theoretical Biology*, 448, 26–37.

Bekcheva, M., Join, C., and Mounier, H. (2018). Cascaded model-free control for trajectory tracking of quadrotors. In *International Conference on Unmanned Aircraft Systems, ICUAS'18*. Dallas, TX, USA.

Birglen, L. and Gosselin, C.M. (2004). Kinetostatic analysis of underactuated fingers. *IEEE Transactions on Robotics and Automation*, 20(2), 211–221.

Birglen, L., Lalibert, T., and Gosselin, C.M. (2010). *Underactuated Robotic Hands*. Springer Publishing Company, Incorporated, 1st edition.

d'Andréa Novel, B., Fliess, M., Join, C., Mounier, H., and Steux, B. (2010). A mathematical explanation via "intelligent" pid controllers of the strange ubiquity of pids. In *18th Mediterranean Conference on Control and Automation, MED'10*, 395–400. doi: 10.1109/MED.2010.5547700.

Fliess, M. and Join, C. (2013). Model-free control. *International Journal of Control*, 86(12), 2228–2252.

Fliess, M. and Join, C. (2021). An alternative to proportional-integral and proportional-integral-derivative regulators: Intelligent proportional-derivative regulators. *Int J Robust Nonlinear Control*, 1–13.

Godage, I., Chen, Y., and Walker, I. (2018). Dynamic control of pneumatic muscle actuators. In *IEEE International Conference on Intelligent Robots and Systems*. Madrid, Spain.

Hamiche, K., Fliess, M., Join, C., and Abouaïssa, H. (2019). Bullwhip effect attenuation in supply chain management via control-theoretic tools and short-term forecasts: A preliminary study with an application to perishable inventories. In *6th International Conference on Control, Decision and Information Technologies, CoDIT 2019*. Vancouver, Canada.

Hamon, P., Chablat, D., and Plestan, F. (2021). A new robotic hand based on the design of fingers with spatial motions. In *ASME 2021 International Design Engineering Technical Conferences and Computers and Information in Engineering Conference*. Online, United States.

Michel, L., Join, C., Fliess, M., Sicard, P., and Chériti, A. (2010). Model-free control of dc/dc converters. In *2010 IEEE 12th Workshop on Control and Modeling for Power Electronics (COMPEL)*. Boulder, CO, USA.

Pham Huy Anh, H. (2010). Online tuning gain scheduling mimo neural pid control of the 2-axes pneumatic artificial muscle (pam) robot arm. *Expert Syst. Appl.*, 37, 6547–6560.

Scaff, W., Horikawa, O., and de Sales, M. (2018). Pneumatic artificial muscle optimal control with simulated annealing. In *10th IFAC Symposium on Biological and Medical Systems BMS 2018*, volume 51, 333–338. Sao Paolo, Brazil.

Sgarbi, F. and Detriche, J.M. (1989). Grab system actuated by a servo motor. European Patent EP0402229.

Takosoglu, J. (2020). Angular position control system of pneumatic artificial muscles. *Open Engineering*, 10(1), 681–687.

Takosoglu, J.E., Laski, P.A., Blasiak, S., Bracha, G., and Pietrala, D. (2016). Determining the static characteristics of pneumatic muscles. *Measurement and Control*, 49(2), 62–71.

Thanh, T.D.C. and Ahn, K.K. (2006). Nonlinear pid control to improve the control performance of 2 axes pneumatic artificial muscle manipulator using neural network. *Mechatronics*, 16(9), 577–587.

Tondu, B. and Lopez, P. (2000). Modeling and control of mckibben artificial muscle robot actuators. *IEEE Control Systems Magazine*, 20(2), 15–38.

Tondu, B. (2012). Modelling of the mckibben artificial muscle: A review. *Journal of Intelligent Material Systems and Structures*, 23, 225 – 253.

Villagra, J., Join, C., Haber, R., and Fliess, M. (2020). Model-free control for machine tools. In *21st IFAC World Congress, IFAC 2020*. Berlin, Germany.

Xu, Q. (2013). Design and smooth position/force switching control of a miniature gripper for automated microhandling. *IEEE Transactions on Industrial Informatics*, 10(2), 1023–1032.

Yeh, T.J., Wu, M.J., Lu, T.J., Wu, F.K., and Huang, C.R. (2010). Control of mckibben pneumatic muscles for a power-assist, lower-limb orthosis. *Mechatronics*, 20(6), 686–697.

Younes, Y., Drak, A., Noura, H., Rabhi, A., and El hajjaji, A. (2014). Model-free control of a quadrotor vehicle. In *2014 International Conference on Unmanned Aircraft Systems, ICUAS 2014*. Orlando, FL, USA.

Zhao, J., Zhong, J., and Fan, J. (2015). Position control of a pneumatic muscle actuator using rbf neural network tuned pid controller. *Mathematical Problems in Engineering*, 2015, 1–16.

Zhong, J., Zhou, X., and Luo, M. (2018). A new approach to modeling and controlling a pneumatic muscle actuator-driven setup using back propagation neural networks. *Complexity*, 2018, 1–9.

Åström, K.J. and Murray, R.M. (2008). *Feedback Systems*. Princeton University Press.